Changes In The Radioactivity, Topography, And Surface Composition Of Uranium After Hydrogen Loading By Aqueous Electrolysis

J.Dash

Low Energy Nuclear Laboratory, Portland State University, Portland, Oregon, U.S.A., dashj@pdx.edu

D. Chicea

Physics Department, University Lucian Blaga of Sibiu,Romania
dan.chicea@ulbsibiu.ro

ABSTRACT

Hydrogen loading of 99.98% pure natural uranium foils (0.18 mm thick) was performed by aqueous electrolysis in order to compare with glow discharge results. Alpha, beta, and gamma specific radioactivity were measured after hydrogen loading and compared with the control. Some of the samples revealed an increase of the specific radioactivity of up to 20%. Gamma ray spectroscopy was also performed on the samples. Results reveal an increase of the specific counts for the peaks of Th234 and U235 and a decrease in the U Kα1 characteristic x-ray peak. The surface topography changed from granular before electrolysis to pitted afterward. The thorium concentration increased slightly after electrolysis compared with the original material. In summary, this work in progress reveals that loading hydrogen into uranium increases the uranium decay rate, in agreement with the glow discharge results.

1 Introduction

This paper describes five experiments that were performed to load hydrogen into natural (not enriched) metallic uranium samples. All samples were taken from the same batch. One sample randomly selected was considered the reference (control) sample and the other five were loaded with hydrogen. The electrolysis parameters are presented in the next section. Non-spectrometric alpha, beta and gamma radioactivity of each sample was measured using a Ludlum Model 3030 alpha-beta counter, and gamma ray spectra were recorded using an ORTEC gamma ray spectrometer. The results of the alpha, beta and gamma counting are presented in section 3. The results of the gamma ray spectrometry are presented in section 4, and the changes in topography and surface composition are given in section 5. These results are discussed in section 6.

2 Hydrogen loading parameters

The cathode was natural uranium foil, 0.18 mm thick, of purity 99.98%. It was obtained from Goodfellow Corp. The electrolyte was H_2SO_4, in deionized H_2O. For S2, DC1 and DC2 the H_2SO_4 which was used was obtained from Alfa Aesar, Stock number 11000, Lot B05119, and the electrolyte was 0.83M. For experiments with cathodes DC3 and DC4 the H_2SO_4 was obtained from J.T. Baker, lot K10030 and the electrolyte was 0.74M. The anode was made of platinum foil, 0.1 mm thick, 99.99% purity (metal basis), Lot Number: 09119EU, obtained from the Aldrich Co. It was a circular platinum disc under the cathode for S2, DC1 and DC2, and had the shape presented in Fig. 1 for DC3 and DC4.

The uranium cathode foil was pierced and the platinum cathode lead wire was bent to make a small hook which is then crimped against the uranium foil. After attaching the cathode to the cathode holder, the electrical contacts for samples DC2, DC3, and DC4 were insulated with 732 Multi-Purpose Silicone Sealant,

(100% silicone rubber), to minimize electrolyte contact with the U-Pt contact. With this design the U-Pt contact corrosion was minimized, thus enabling prolonged electrolysis.
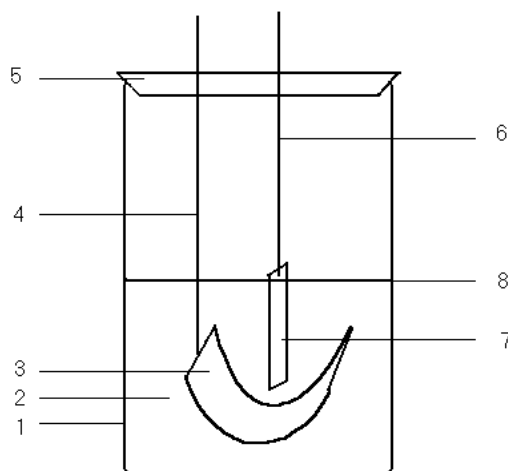
The cell design is presented in Fig. 1 where the numbers represent:

1. Beaker (200 ml, Pyrex)
2. Electrolyte
3. Pt Anode
4. Anode Pt holder
5. Teflon cap
6. Pt cathode holder
7. Uranium foil cathode
8. Electrolyte level

With this cell five experiments were conducted. Experiments labelled as S2 and DC1 did not have insulation covering the electric contact between the platinum cathode lead wire and the cathode, while DC2, 3 and 4 had the electrical contact insulated. The electrolysis parameters are summarized below.

Table 1. *Current, voltage, current density and electrolysis time for the five experiments.*

Experiment	Current, A	Voltage, V	Current density, mA/cm^2	Electrolysis time, h
S2	1.5	4.0	1781	5
DC1	0.075	3.0	50	72
DC2	0.4	2.9	370	206
DC3	0.035	2.4	26	65
DC4	0.15	2.5	54	66

3 Non - spectrometric alpha, beta, and gamma radioactivity measurement

The samples were weighed and radioactivity was measured with a Ludlum Model 3030 Alpha-Beta Sample Counter, having an organic scintillator in a shielded chamber and a pulse-height analyzer that provides information to two independent counters. The counter has a RS232 interface that enables data acquisition and operating parameters control and adjustment using a PC. The counter was used in the scaler mode. The count accuracy of the detection system is 2%, as stated by the manufacturer.

Each sample was weighed before and after the experiment using a Mettler model H70 balance. After that the samples were cut in such a manner that the parts that were above the electrolyte level were separated from the parts that were below the electrolyte level. The parts that were above were labeled with a trailing P1a

while those that were under the electrolyte during the experiment were labeled with a trailing P2u. In addition to the α and β counts that the Ludlum Model 3030 counter provides, γ radioactivity was measured as well. In order to do a γ radioactivity measurement the sample was completely covered with an aluminum plate 0.9 mm thick. The aluminum plate completely absorbed α particles and statistically almost all of the β particles. Therefore the counts on the β channel with the aluminum plate between sample and detector are proportional to the γ activity of the sample.

For each sample the background on both alpha and beta channels was measured before the counting and was subsequently subtracted, and the specific radioactivity, that is counts per second per gram, was calculated. The results of the measurements performed with the Ludlum counter for the two parts of the sample are presented in Table 2. Variation is defined as electrolyzed sample radiation minus control sample radiation divided by control radiation.

Table 2. *Alpha, beta and gamma radiation and variation for the five samples and control*

Sample	Specific alpha, c/g*s	Alpha variation, %	Specific beta, c/g*s	Beta variation, %	Specific gamma, c/g*s	Gamma variation, %
S1	97		2210		545	
S2P1a	142	47.2	2711	22.7	640.7	17.5
S2P2u	115	19	2470	11.8	595	9.1
DC1P1a	158	63.4	2726	23.4	660	21
DC1P2u	124	28.7	2354	6.5	580	6.3
DC2P1a	107	11.1	2338	5.8	581	6.5
DC2P2u	128	33.1	2542	15	617	13.1
DC3P1a	115	19.5	2345	6.1	583	6.9
DC3P2u	110	13.9	2514	13.8	599	9.8
DC4P1a	115	19	2407	8.9	543	-0.5
DC4P2u	120	24.8	2317	4.9	576	5.6

The data presented in Table 2 is plotted in Figures 2 and 3. Examining Table 2 and Figures 2 and 3, we notice that alpha variation is bigger than beta, and beta is bigger than gamma variation. We also notice that for sample S2 and DC1 (no insulation on cathode contact), the part that was above the electrolyte has a bigger increase of the specific radioactivity for all the three types of radioactivity than the part that was under electrolyte, while for the samples DC2 through DC4 (insulated cathode contact) the results show the opposite.
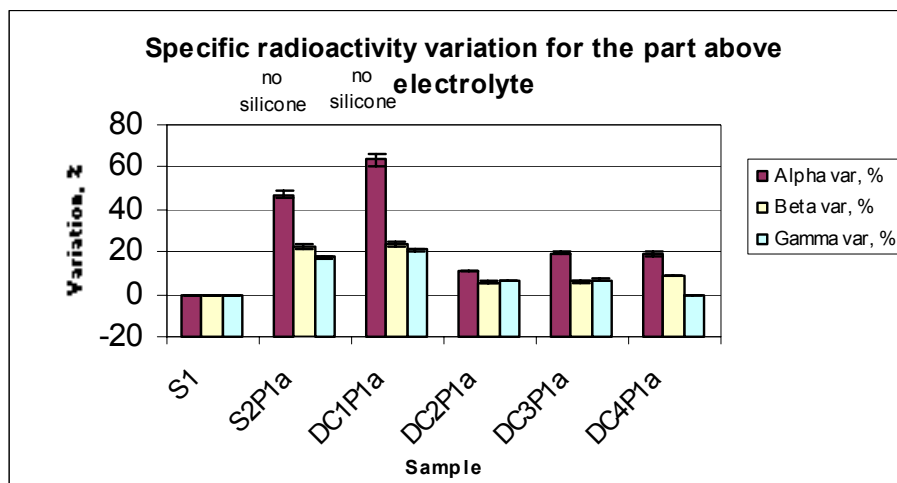

Fig. 2. The variation of the specific alpha, *beta and gamma radioactivity of the part that was above electrolyte, compared with the reference sample* S1.
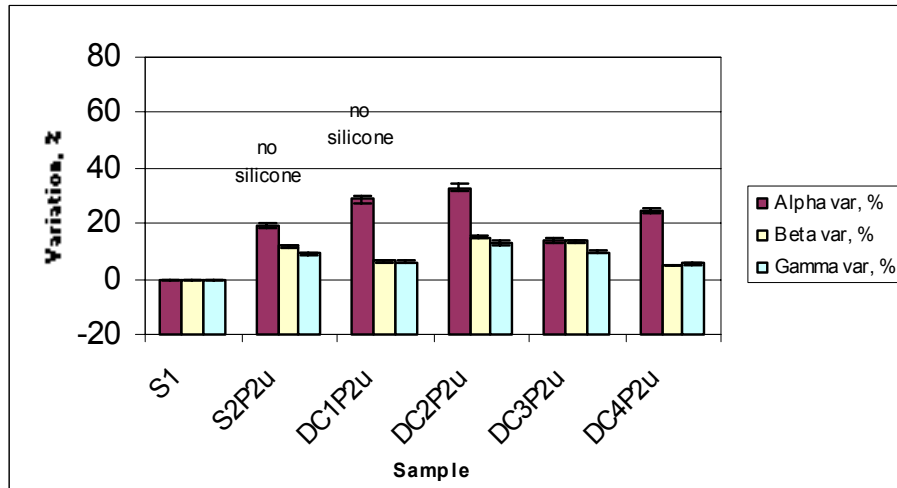
Fig. 3. *The variation of the specific alpha, beta and gamma radioactivity of the part that was under electrolyte, compared with the reference sample* S1.

4 Gamma ray spectroscopy results

The gamma spectra were acquired using an ORTEC gamma ray spectrometer with 8000 channels and a germanium detector cooled to liquid nitrogen temperature. The spectra were analyzed with Gammavission-32 software. Each sample was placed in a plastic dish and counted for one hour on each of the sides, and the data was averaged. The data averaged for the two sides of each part of each sample, divided by the mass, therefore expressed in gamma counts per gram - hour, are presented in Tables 3 and 4.

Table 3. *Specific (counts per gram-hour) gamma and characteristic x-ray data for control and for the portions of the samples above electrolyte.*

Line / Sample	S1	S2P1a	DC1P1a	DC2P1a	DC3P1a	DC4P1a
92.4 keV Th234	276898	302659	300854	277542	270147	268015
98.5 keV U Kα1	131785	122452	119314	128507	129092	131300
186 keV U235	108863	118427	116934	109603	106548	108958

Table 4. *Specific (counts per gram-hour) gamma and characteristic x-ray data for control and for the portions of the samples below electrolyte.*

Line/Sample	S1	S2P2u	DC1P2u	DC2P2u	DC3P2u	DC4P2u
92.4 keV Th234	276898	288293	288892	295887	291973	274560
98.5 keV U Kα1	131785	127667	132771	128026	126001	129023
186 keV U235	108863	112547	114350	116630	113957	109334

Among the gamma lines and the characteristic x-ray lines, the Th[234] 92.4 keV gamma line, U 98.5 keV Kα1 x-ray, and U[235] 186 keV gamma line counts are measured with the smallest error. Therefore, they were selected to be presented. The plots of specific counts for the samples, measured separately for the part that was above electrolyte or under electrolyte, expressed in counts/gram*hour, are presented in Figures 4 through 6.
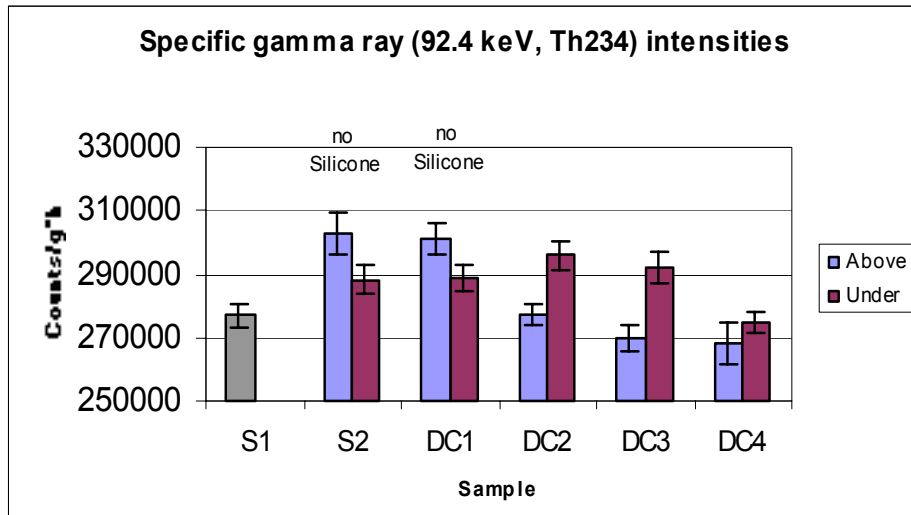
Fig. 4. *92.4 Th^{234} keV gamma ray specific intensity for the electrolysed uranium samples compared with the control*

Examining Figure 4 we notice that for S2 and DC1, hydrogen loading produced a significant increase of the specific 92.4 Th^{234} keV gamma ray emission and for the other three samples the variation is within the experimental error, for the parts of the samples above electrolyte. Four of the parts that were under direct hydrogen exposure, that is under electrolyte, present a significant increase of the specific 92.4 Th^{234} keV gamma ray emission while one (DC4) has no significant variation.

Figure 5 shows that both parts of samples S2, DC2, and DC3 present a decrease of the 98.5 keV uranium Kα1 characteristic x-ray specific counts. The portion of DC1 above the electrolyte level has about 10% lower intensity than the control, but the portion below has the same intensity as the control. Both parts of DC4 have about the same intensity as the control. Figure 6 reveals that U^{235} gamma ray specific radioactivity increased as a result of hydrogen loading for both parts of S2 and DC1 and for the parts of DC2 and DC3 which were below the electrolyte level. It was not modified for DC4.
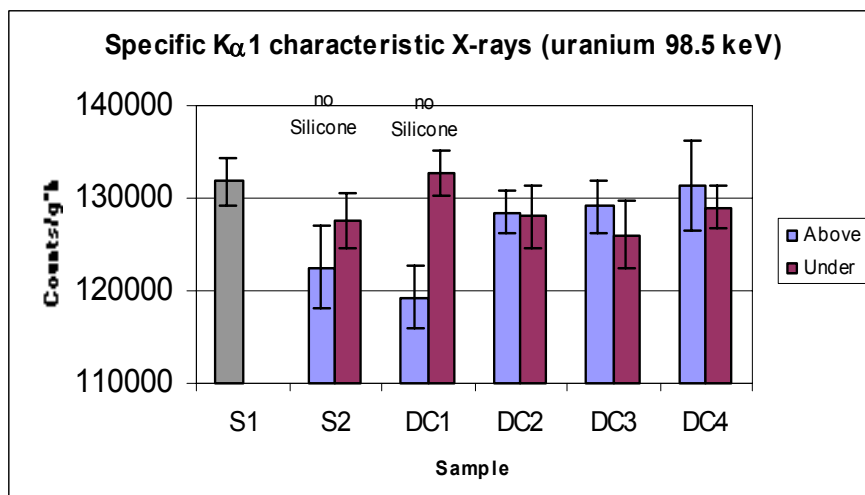

Fig. 5. *Kα1 98.5 keV uranium characteristic x-ray specific intensity for the electrolyzed uranium samples compared with the control*
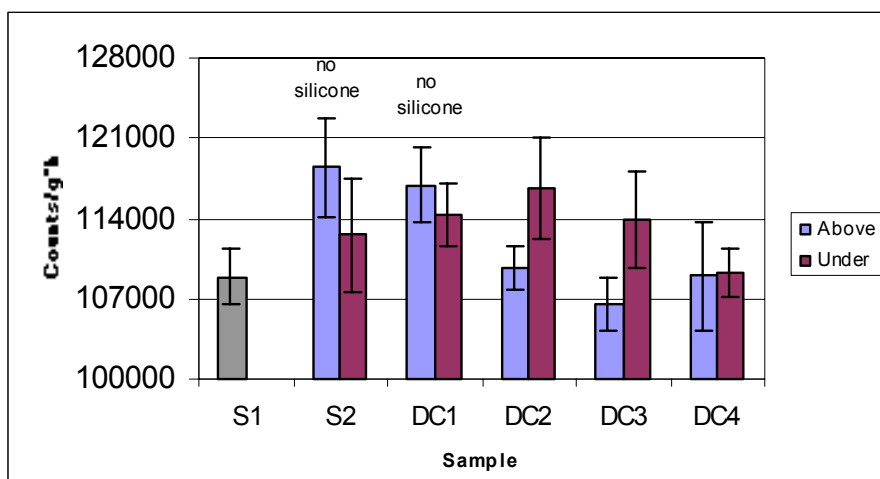
Fig. 6. 186 *keV U^{235} gamma ray specific intensity for the electrolysed uranium samples compared with the control (S1).*

5 Topography and surface composition

Changes in surface morphology which resulted from electrolysis were determined with a scanning electron microscope (SEM), and changes in surface chemical composition were determined with an energy dispersive spectrometer (EDS) attached to the SEM.

A typical image of the natural uranium surface before electrolysis is presented in Fig. 7. The surface is nonuniformly fissured and granulated, with granule sizes up to 3-4 µm.
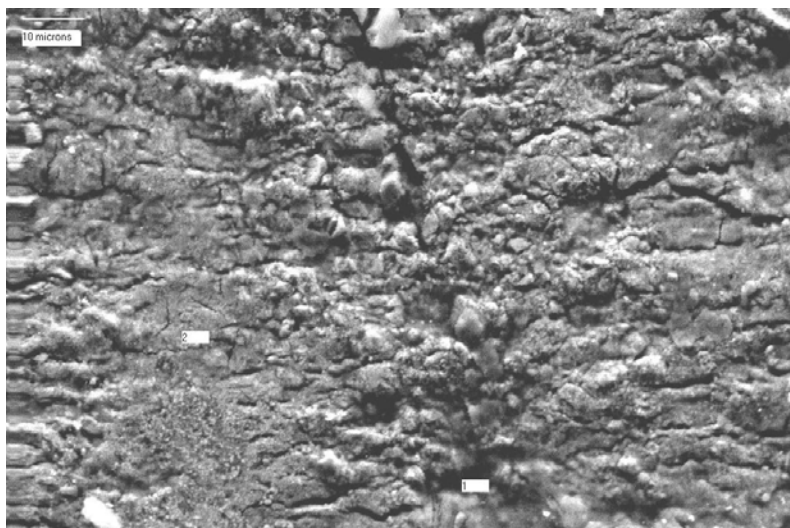

Fig. 7. Magnified image of the unelectrolyzed natural uranium surface magnified image of the unelectrolyzed natural uranium

Sample DC1 was electrolyzed and analyzed following the same procedure, that is taking a low magnification image first, then high magnification images and spectra from several locations. A magnified image of the surface of sample DC1, after absorbing hydrogen, is presented in Fig. 8. Sample DC1 presents evidence of pitting, which may have been caused by the formation of uranium hydride and erosion. The surface is covered with pits having a typical size of about 1 μm. The main difference in the topography of the surface is that on the unelectrolyzed natural uranium sample surface the granules protrude above the surface while on the electrolysed sample the surface is pitted.
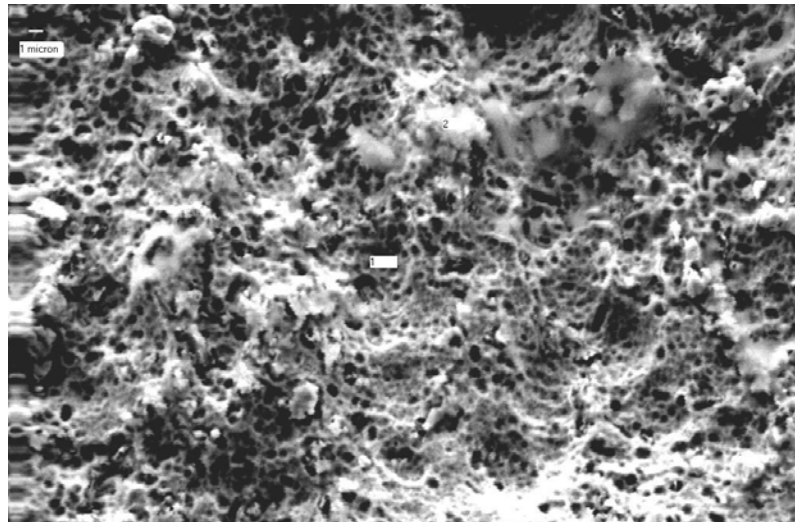

Fig. 8. *A magnified image of the DC1 uranium surface after hydrogen loading by electrolysis.*

The concentrations of thorium and carbon were measured on an as-received natural uranium sample (the control) and on each sample after electrolytic loading with hydrogen. The concentration data were obtained with an Oxford Model 5565 EDS, attached to an ISI Model SS40 SEM. The data presented in the tables and the standard deviations, hereafter sigma, are atomic concentrations.

First only thorium and uranium were selected on the list for the quantitative analysis. Table 5 presents the average values of thorium concentrations and the average standard deviations (σ).

Table 5. *Average thorium concentration and standard deviation for the control natural uranium sample (S1) and for the samples that were loaded with hydrogen.*

Sample	Th (%)	σ Th (%)	Number of spectra	Average counts for each spectrum
S1(control)	0.96	0.43	14	480321
DC1	1.05	0.37	13	537439
DC2	1.24	0.43	13	522777
DC3	1.95	0.68	10	180598
DC4	1.56	0.63	23	583748

The averages are calculated for each sample separately. Table 5 shows that there is an increase of the thorium concentration for the hydrogen-loaded uranium samples compared with the control, but the increase is smaller than one sigma. All of the thorium concentrations in Table 5 exceed two standard deviations, so the results are significant.

The carbon concentrations on the sample surfaces were also determined by EDS. Table 6 presents the average values of the surface carbon content and the average standard deviations for each sample. Examining Table 6, we notice first that the carbon concentrations are significantly larger than two standard deviations. All

of the electrolysed samples have significantly less carbon than the unelectrolyzed control. The origin of this carbon is not known.

Table 6. *Carbon average concentrations and standard deviations for the control natural uranium sample (S1) and for the samples that were loaded with hydrogen.*

Sample	C (%)	σ C (%)	Number of spectra	Average counts
S1 (control)	59.79	0.88	13	775233
DC1	51.28	0.81	15	469438
DC2	42.76	0.56	16	500043
DC3	32.54	0.71	11	187373
DC4	34.57	0.93	23	583748

The data presented in Tables 5 and 6 is plotted in Figures 9 and 10, respectively.

When examining the Tables 5 and 6, we should be aware that the concentrations that are written on the SEM analysis sheet are not the absolute concentrations. For example, 1% Th means that the ratio Th/U is 1/99, and 50% C means that the ratio C/U is 50/50, etc. Another important point is that the EDS analysis gives the composition of the surface to a depth of about 1 μm, since a 20 keV electron beam is used.
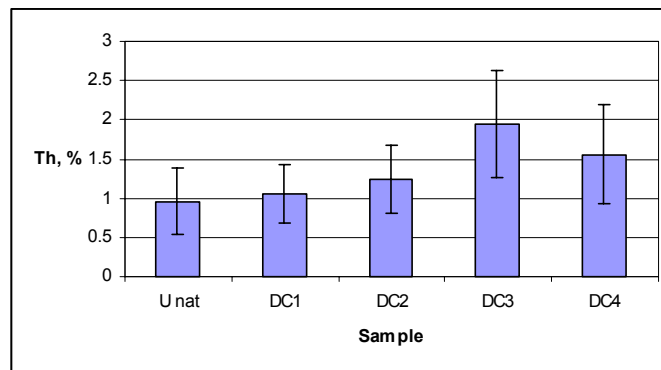

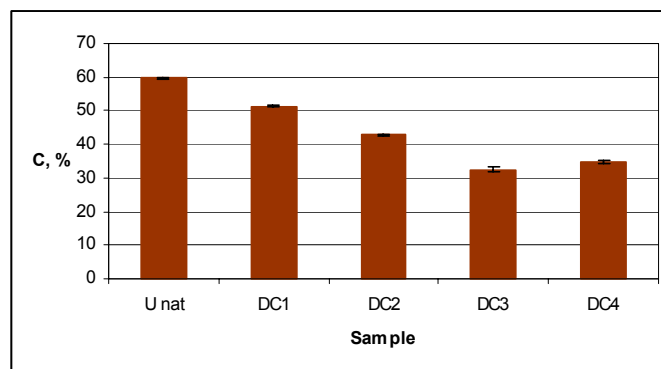Fig. 9. *Thorium concentration for electrolyzed samples compared with the control (Unat).*

Fig. 10. *Surface carbon concentration for the electrolyzed samples compared with the control,Unat contro*
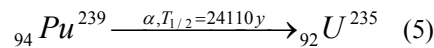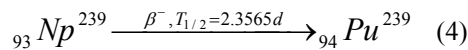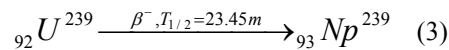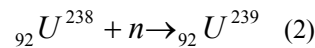
6 Discussion

The results of the experiments of loading hydrogen into natural uranium samples using electrolysis reveal that the intensity of the alpha radioactivity of the samples increased after loading hydrogen, both for the parts that were located under electrolyte and above electrolyte. The same result was found for the beta radioactivity. The gamma radioactivity increased for the parts of the samples that were under electrolyte for all the samples and for the parts that were above electrolyte for four out of five samples, and was not modified for one of the samples. These results show with a precision that is well above the experimental errors that the alpha, beta and gamma radioactivity of the natural uranium samples increased as a result of absorbing hydrogen.

Gamma ray spectrometry revealed that for the majority of the samples the intensity of the 92.4 keV Th^{234} gamma line increased, the intensity of the 186 keV U^{235} increased and the intensity of the 98.5 keV uranium $K\alpha1$ characteristic x-ray peak decreased. The atomic electron excitations are produced primarily by the alpha particles emitted by U^{238} decay. The alpha emission proved to be more intense but the uranium characteristic x-ray intensity decreased. This suggests that the uranium concentration in the electrolyzed sample decreased while the U^{235} and Th^{234} concentrations increased. Th^{234} follows U^{238} directly in the U^{238} decay chain, as presented in equation 1. The half life is 24.10 days [1]. The increase of Th^{234} concentration suggests that the U^{238} decay rate has been increased as a result of hydrogen absorption.

$$_{92}U^{238} \xrightarrow{\ 4.468E+9\ y\ } _{90}Th^{234} \quad (1)$$
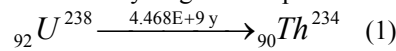
A set of nuclear reactions that might explain the increase of the U^{235} concentration, under the assumption that the decay rate stated in equation 5 is increased, might be:

$$_{92}U^{238} + n \rightarrow _{92}U^{239} \quad (2)$$

$$_{92}U^{239} \xrightarrow{\ \beta^-, T_{1/2}=23.45m\ } _{93}Np^{239} \quad (3)$$

$$_{93}Np^{239} \xrightarrow{\ \beta^-, T_{1/2}=2.3565d\ } _{94}Pu^{239} \quad (4)$$

$$_{94}Pu^{239} \xrightarrow{\ \alpha, T_{1/2}=24110y\ } _{92}U^{235} \quad (5)$$

The half life of the isotopes in equations 2 through 5 are taken from [2 - 6]. The nuclear reaction in equation (2) is suggested in [7] and the reaction mechanism in [8].

These results are very similar to those reported in [9] and [10] where the gamma ray spectrometry and thermal ionization mass spectrometry results reveal a 1% decrease of the uranium concentration in the samples that were exposed to hydrogen isotope plasma. In order to verify that the U^{238} half life has been decreased, measurements must be taken periodically over a time interval of years to check whether the alpha radioactivity remains increased and whether the Th^{234} gamma activity remains higher than for the reference sample. Another way to verify that the U^{238} decay rate has increased for all the isotopes in the U^{238} decay chain would be to measure the Pb^{206} to Pb^{204} ratio by mass spectrometry in both the electrolysed samples and the reference sample. If it is higher in the electrolyzed sample than in the reference sample, then the whole U^{238} chain decay rate has been increased by hydrogen absorption. This result was already obtained for uranium exposed to hydrogen isotope plasmas [10].

References

[1] A.M.Sanchez, P.R.Montero , Simplifying Data Fitting using Branching Ratios as Constraints in Alpha Spectrometry, Nucl.Instrum.Methods Phys.Res. A420, 481 (1999)

[2] A.Lorenz , Decay Data of the Transactinium Nuclides , IAEA Tech.Rept.Ser., No.261, 1986.

[3] S.A.Woods, D.H.Woods, M.J.Woods, S.M.Jerome, M.Burke, N.E.Bowles, S.E.M.Lucas, C.Paton Walsh, Standardization and Measurement of the Decay Scheme Data of ^{243}Am and ^{239}Np, Nucl.Instrum.Methods Phys.Res. A369, 1996, p. 472.

[4] D.Sardari, T.D.Mac Mahon, S.P.Holloway , ^{239}U and ^{243}Am Decay Data, Nucl.Instrum.Methods Phys.Res. A369, 1996, p. 486.

[5] G.T.Ewan, J.S.Geiger, R.L.Graham, D.R.MacKenzie, Conversion Electron Spectrum of Np^{239} and Level Scheme of Pu^{239}, Phys.Rev. 116, 1959, p. 950.

[6] A.M.Sanchez, P.R.Montero , Simplifying Data Fitting using Branching Ratios as Constraints in Alpha Spectrometry, Nucl.Instrum.Methods Phys.Res. A420, 1999, p. 481.

[7] J.J. Dufour, J.H. Foos, X.J.C Dufour, Formation and Properties of Hydrex and Deutex, Conf. Proce. Vol 64, Anomalies in Hydrogen/Deuterium Loaded Metals, S.I.F., Bologna, 1999, p. 29.

[8] H. Kozima, K. Arai, Local Coherence, Condensation and Nuclear Reaction of Neutrons at Crystal Boundary of Metal Hydrides and Deuterides, Int. J. Hydrogen Energy 25 (9), 2000, p. 845.

[9] J. Dash, I. Savvatimova, S. Frantz, E. Weis, and H. Kozima, Effects of Glow Discharge with Hydrogen Isotope Plasmas on Radioactivity of Uranium, Proc. of the 9th International Conference on Cold Fusion, Beijing, p. 77, 2002.

[10] J. Dash, I. Savvatimova, S. Frantz, E. Weis, Effects of Glow Discharge with Hydrogen Isotope Plasmas on Radioactivity of Uranium, submitted for publication.